

N 79-17520

MEASUREMENT OF HUMAN ANKLE JOINT COMPLIANCE  
USING RANDOM TORQUE INPUTS

Gyan C. Agawal  
Gerald L. Gottlieb

College of Engineering  
University of Illinois at Chicago Circle  
Chicago, Illinois 60620

and

Department of Physiology  
Rush-Presbyterian-St. Luke's Medical Center  
Chicago, Illinois 60612

ABSTRACT

The compliance of the human ankle joint is measured by applying 0 to 50 Hz band-limited Gaussian random torques to the foot of a seated human subject. These torques rotate the foot in a plantar-dorsal direction about a horizontal axis at a medial malleolus of the ankle. The applied torques and the resulting angular rotation of the foot are measured, digitized and recorded for off-line processing. The data are analyzed by computing the auto-power and cross-power spectra of the angle and the torque using 4.096 second data records with 2.048 seconds of overlap between successive records. For 30 seconds of data, approximately 15 sets of spectra are computed and averaged. From these averages, the transfer function of compliance (ratio of angle to torque) is computed as is the coherence function. High values of coherence in the frequency range of 2 to 30 Hz and well-behaved compliance and phase curves suggest that the system may be reasonably approximated by a second-order linear-differential equation. Using such a best-fit, second-order model, the effective moment of inertia of the ankle joint, the angular viscosity and the stiffness are calculated.

The ankle joint stiffness is shown to be a linear function of the level of tonic muscle contraction, increasing at a rate of 20 to 40 Nm/rad/Kg.m. of active torque. In terms of the muscle physiology, the more muscle

fibers that are active, the greater the stiffness. Joint viscosity also increases with activation. Joint stiffness is also a linear function of the joint angle, increasing at a rate of about 0.7 to 1.1 Nm/rad/deg from plantar flexion to dorsiflexion rotation.

INTRODUCTION

The design and development of devices for rehabilitation of paralyzed and paretic patients would be facilitated by more accurate knowledge about the dynamic response of the joint under control (1). For example, simple devices have been proposed for correcting foot drop by functional electrical stimulation (2).

The measurement of mechanical impedance in biomechanical systems has diverse applications. Many workers have used such measurements to study the vibration response of the whole body (3,4,5), the head (6), the knee (7) and the hand-arm system (8,9). The impedance concept has been used to assess the type and degree of ligamentous injury to the knee (7), to determine the moment of inertia of a limb segment (10) and to measure muscle tone (11).

Mechanical impedance is measured by applying a disturbance and measuring the appropriate force and displacement variables. In the absence of conscious intervention on the part of the subject, a limb will resist an externally applied torque. This resistance will have three components: 1) passive inertia about the joint; 2) visco-elastic stiffness of the joint and the muscles which act about it; and 3) the reflex contraction of stretched muscles.

The first of these may be presumed constant although it is somewhat a function of joint angle. The second is a function of the level of muscle activation (12). The third is time-varying and is sensitive to influences from a host of central nervous processes.

Reflex effects, which directly influence the level of muscle activation will consequently alter the visco-elastic properties of the muscle. Even if we exclude voluntary changes in innervation, we are still dealing with mechanisms which are adaptive with relation to external disturbances.

D45

The rotation caused by external torques may be characterized as the joint compliance. Several techniques have been used for its measurement. One approach is to apply impulses of torque and measure the mechanical and electrical responses (13, 14). A disadvantage of this technique is that such stimuli may be "unphysiological" and the results difficult to extrapolate to other less stressful inputs. A second approach is to apply sinusoidal disturbances over a range of frequencies (8, 9, 15, 16). Predictions of the responses to other classes of input signals can then be made if the system is sufficiently linear to allow the principal of superposition to be applied. A third approach is to apply a relatively wideband, gaussian torque input covering the frequency spectrum of significant system dynamics.

Although linearity of the motor system has not been established, linear analysis has proven to be a versatile tool in describing components of the motor system such as muscle (17, 18), the muscle spindle (19, 20) and the integrated system (13, 14, 21, 22).

In this paper we will consider the measurement of ankle joint compliance using a band-limited gaussian torque disturbance and compare the responses with our earlier work using impulse torque inputs (tendon-jerk response) and sinusoidal torque inputs (13, 16). Muscle properties are known to be dependent on the level of active contraction (12) and on the length of the muscle (23). Consequently, we have examined joint compliance as a function of the muscle contraction and the mean angular operating point.

#### METHODS

These experiments have been done on over twelve normal, adult, male human subjects. A subject sat in a chair with the right foot strapped to a footplate which could rotate about a horizontal, dorsal-plantar axis through the medial malleolus. A schematic of the equipment used is shown in Figure 1.

The plate could be rotated by a D.C. torque motor (Inertial Motors Corp. No. 06-024) via a gearbelt and pulley system for torque amplification. Constant tension springs are also used to counter-balance the planter gravitational torque. With the subject completely relaxed, the resulting joint position (approximately 90° between the foot and the tibia) defines a reference ankle position. A dual beam oscilloscope provides the subject with visual feedback of foot angle on one channel and the reference position on the other.

A band-limited gaussian (0-50 Hz) signal was prerecorded from a noise generator.

In the first experiment, these time-varying signals were superimposed on a mean motor torque level.

The applied torque was controlled via a torque servo-mechanism.

The subject was instructed to try to maintain a constant mean force against the bias

torque of the motor so that foot movement was nearly symmetrical with respect to the reference angle.

This was accomplished with little difficulty by all subjects. The input was applied for 30 sec or more and the data continuously recorded on a digital tape.

In the second experiment, with the subject completely relaxed, a biasing torque was added to displace the resting position of the foot

in the dorsal or plantar direction and another 30 second measurement

was made. This procedure was repeated for various angles over a range

of about 12° in each direction about a neutral position.

Bias torques were then added to the gaussian signal and the subject was instructed

to counteract them by keeping the motion of his foot centered about

the visual reference.

The torque was measured by a strain gauge bridge on the side arms

of the foot-plate. Angular rotation was measured by a continuous

potentiometer. Electromyograms (EMG) were recorded from disc surface

electrodes placed over the bellies of the gastrocnemius-soleus (GS) and

the anterior tibial (AT) muscles. These were amplified, full-wave

rectified and filtered (10 msec averaging time) before recording. A

digital computer (General Automation SPC - 16/65) generated the motor

drive voltage at a conversion rate of 250/sec and digitized data on

four channels. The angle and the torque signals were sampled at a rate

of 250/sec and the filtered EMG at a rate of 500/sec.

The data was analyzed by computing the autopower and crosspower spectra of the angle and torque records using 4,096 second data records (1024 points) and a cosine taper (24) with 2,048 seconds of overlap between successive records. For 30 seconds of data, approximately 15 sets of spectra were computed and averaged.

Transfer functions were computed by the following method. Let  $S_r(j\omega)$  and  $S_\theta(j\omega)$  denote the Fourier transform (FFT) of torque and angle. The average auto and crosspower spectra are given by:

$$G_{rr}(\omega) = \frac{S_r(j\omega) S_r(-j\omega)}{S_r(j\omega) S_r(-j\omega)}$$

$$G_{\theta\theta}(\omega) = \frac{S_\theta(j\omega) S_\theta(-j\omega)}{S_\theta(j\omega) S_\theta(-j\omega)}$$

$$G_{\theta r}(\omega) = \frac{S_\theta(j\omega) S_r(-j\omega)}{S_\theta(j\omega) S_r(-j\omega)}$$

These were computed as ensemble averages using the transformed data  $S_r(j\omega)$  and  $S_\theta(j\omega)$ .

The transfer function of compliance (ratio of angle to torque) is given by

$$\text{Joint Compliance} = \frac{G_{\theta r}(\omega)}{G_{rr}(\omega)}$$

and the coherence function is defined as

$$\gamma^2 = \frac{G_{\theta r}(j\omega) G_{\theta r}(-j\omega)}{G_{rr}(\omega) \cdot G_{\theta\theta}(\omega)}$$

The coherence function lies between zero and one. For a linear noise free system it is equal to one.

## RESULTS

The application of bandlimited Gaussian torque (0 to 50 Hz) produces a response such as illustrated in Figure 2. The angular rotation shows that the torque input has been significantly lowpass filtered by the mechanical and neuromuscular properties of the limb.

Considerable electromyographic activity can be seen in both muscles. In this record, the gastrocnemius-soleus muscles were undergoing voluntary, tonic contraction opposing a motor bias torque of 0.26 Kg.m. The RMS value of the gaussian torque was 0.20 Kg.m.

The effective compliance of the ankle joint as a function of frequency is shown in Figure 3. This shows the results for the relaxed limb and at bias torque levels of 0.13 and 0.26 Kg.m. Figure 4 shows the corresponding phase relationship (foot angle always lags the applied torque). Figure 5 shows the measured coherence functions for this experiment.

The high values of coherence in the frequency range of 2 to 30 Hz, and well-behaved compliance and phase curves suggest that the system may be reasonably approximated by a second-order, linear differential equation with constant coefficients. The solid lines drawn in Figure 3 are from a best-fit, second order model:

$$\text{Joint Compliance} = \frac{\theta}{r} = \frac{1}{JS^2 + BS + K}$$

where:

$J$  = moment of inertia of the foot and the plate with respect to the axis of rotation through the medial malleolus (in N.m.sec<sup>2</sup>/rad)

$B$  = angular viscosity coefficient (in N.m.sec/rad)

$K$  = angular stiffness (in N.m/rad)

$S$  = Laplace transform complex frequency

The criterion used for the model fit was:

$$\text{Error} = \sum_f \left[ \log \left( \frac{\text{Model Compliance}}{\text{Measured Compliance}} \right) \right]^2$$

Table 1 shows the values of  $J$ ,  $B$ , and  $K$  as well as the damping factors ( $\zeta$ ) and natural frequencies ( $\omega_n$ ) for three subjects as the bias torque is varied. The RMS value of the gaussian torque was kept at 0.2 Kg.m. throughout these runs. The bottom lines in this table show the mechanical parameters of the foot plane system.

As one would expect, the moment of inertia is independent of the bias torque. The mean values for these three subjects are 0.0157, 0.0180, and 0.0186 N.m.sec<sup>2</sup>/rad. Of this inertia, 0.0097 N.m.sec<sup>2</sup>/rad is from the apparatus leaving 0.0060, 0.0083 and 0.0089 N.m.sec<sup>2</sup>/rad for the foot. These values are comparable to the values of 0.0107 N.m.sec<sup>2</sup>/rad for an average male subject calculated by Hogins (25) by considering serial sections of the foot from anatomical data and of 0.024 N.m.sec<sup>2</sup>/rad calculated by Trunkoczy et al. (1) by considering foot as a prism. (Hogins' estimates of moment of inertia after correcting for the body weight and foot length for the first two subjects are 0.0074 and 0.0102 N.m.sec<sup>2</sup>/rad, respectively).

The viscous coefficient and the stiffness are clearly functions of the bias torque. These variables are plotted in Figure 6.

The solid lines are the first order, least square regression lines. The equations of these regression lines for the three subjects are:

$$\begin{aligned} K: & 23.3r_B + 22.5 \quad (0.992) \\ & 40.5r_B + 15.3 \quad (0.996) \\ & 38.9r_B + 14.9 \quad (0.999) \\ B: & 0.161r_B + 0.363 \quad (0.891) \\ & 0.332r_B + 0.237 \quad (0.915) \\ & 0.143r_B + 0.412 \quad (0.666) \end{aligned}$$

where  $r_B$  is the bias torque. The correlation coefficients are given in the parentheses in each case.

Figures 7, 8 and 9 show the ankle joint compliance, phase angle and the coherence function respectively for a case of zero bias torque at three different mean joint angles. The solid lines plotted in Figures 7 and 8 are for the best second-order fit.

Joint stiffness as a function of the mean joint angle is shown in Figure 10 for one subject at three different levels of bias torques. The solid lines are the first order, least squares regression lines. The equations of these lines are:

$$\begin{aligned} r_b = 0 \text{ Nm}, K = 20.3 + 0.695\bar{\delta} \quad (0.931) \\ r_b = 1.1 \text{ Nm(D)}, K = 41.1 + 0.788\bar{\delta} \quad (0.823) \\ r_b = 2 \text{ Nm(P)}, K = 40.4 + 1.12\bar{\delta} \quad (0.903) \end{aligned}$$

Where  $r_b$  is the bias torque and  $\bar{\delta}$  is the mean joint angle in degrees. The correlation coefficients are given in parentheses in each case.

The viscous coefficient for this experiment is given by the following regression lines for the three cases:

$$\begin{aligned} r_b = 0 \text{ Nm}, B = 0.504 + 0.014\bar{\delta} \quad (0.960) \\ r_b = 1.1 \text{ Nm(D)}, B = 0.595 - 0.001\bar{\delta} \quad (-0.215) \\ r_b = 2 \text{ Nm(P)}, B = 0.675 + 0.013\bar{\delta} \quad (0.793) \end{aligned}$$

All other subjects tested for this experiment (four in all), showed similar behavior in the relationship of  $K$  vs.  $\bar{\delta}$ . That is, in the relaxed limb there was a monotonic change in  $K$  over the range of about  $\pm 12^\circ$  from neutral and voluntary contractions shifted the curve vertically. Angles greater than  $12^\circ$  were not systematically examined but as the angle increased beyond about  $12^\circ$  in either dorsiflexion or plantarflexion, the stiffness of the ankle increased due to passive mechanical properties of the joint.

#### DISCUSSION

At frequencies above 10 Hz, the foot and footplate offer an inertial load to the applied torque. At the low end of the spectrum, the limb acts like a spring. The spring constant is a linear function (FIG. 6) of the level of tonic contraction, stiffness increasing at a rate of 20 to 40 N.m./rad/kg.m. of active torque. This is a well known finding (see Wilkie (12) for human arm muscle and Joyce and Beck (26) for cat soleus).

The basis for the elastic coefficient being a function of activation lies in the physiology of muscle. The length-tension relationship of the muscle sarcomere indicates that at presumed physiological muscle lengths, an active muscle fiber will increase its contractile tension in a

"spring-like" manner when stretched. An inactive muscle fiber will produce negligible tension. As a consequence, the more muscle fibers that are active, the greater the muscle stiffness.

The values of  $B$  and  $K$  for the ankle joint obtained in these experiments compare reasonably well with the data obtained in other studies. Trakoczy, et al. (1) report  $B = 1 \text{ N.m.sec/rad}$  and  $K = 7.5 \text{ N.m/rad}$  for the human ankle joint. Stark et al. (27) in their experiments on the human arm pronator and supinators found  $B$  and  $K$  increasing with voluntary tension, the values obtained were  $B = 0.0001$  to  $0.0003 \text{ N.m.sec/rad}$  and  $K = 0.02$  to  $0.60 \text{ N.m/rad}$ . The same experiment was repeated by Agarwal et al. (13) and their values were  $B = 0.009$  to  $0.056 \text{ N.m.sec/rad}$  and  $K = 1.05$  to  $6.66 \text{ N.m./rad}$ .

Ishida and Umetani (28) found  $B = 1.5 \text{ N.m.sec/rad}$  and  $K = 21 \text{ N.m/rad}$  for the human upper arm. Fig. 10 indicates that over a range of  $\pm 12^\circ$  on either side of the neutral position, the joint stiffness is linearly dependent on the angular position increasing at a rate of about  $0.7$  to  $1.1 \text{ N.m/rad/degree}$  of mean angular rotation. Most of this dependence can be accounted for by the passive properties of the joint. The same functional angular dependence exists at all levels of muscle contraction and is small compared to the effects of contraction itself.

The use of random torque excitation for measuring joint compliance provides a description of the ankle joint which differs in at least two very distinct ways from the description obtained with sinusoidal torque excitation (15, 16, 29). Within the 5-8 Hz region of the spectrum, sinusoidal torques produce a strong and narrow resonance with a frequency which is dependent on the level of tonic muscle contraction. The resonance is not evident with random torque. Within the 8-12 Hz region, foot rotation often becomes highly non-sinusoidal. Up to 80% of the angular signal power may be at frequencies other than the excitation frequency, particularly at  $\frac{1}{2}$  the excitation frequency. Such nonlinearities are also not evident here.

In both of these phenomena, the stretch reflex is very likely playing an important role when the excitation is sinusoidal. The contribution of the stretch reflex when the excitation is gaussian is not clear. A number of studies of human muscle (1, 18, 30, 31, 32) using widely differing methods have shown that the bandwidth of large muscles functioning as isometric torque generators is only 2 to 3 Hz. Given this sluggish response together with the 50 msec neural transport delay around the reflex arc could indicate that reflexes play a small role when random torques are used.

However, reflex activation of muscle not only produces torque by excitation-contraction processes, it also alters muscle compliance and the dynamics of these compliance changes are not known. It is probable that reflex activation of the muscle by spectral components of the random torque above 5 Hz would increase the stiffness of the muscle to spectral components below 5 Hz. Such an interaction would be quite complex and could account for some of the differences between random and sinusoidal measurements.

There is no question that the neuromuscular systems about the ankle joint are both non-linear and adaptive. The data in this report show that under the present experimental conditions, the system resembles a simple, linear one. Such a description, if taken literally can lead to many false impressions about the functioning of the motor system and extrapolation of these results to other classes of inputs or experimental conditions must be done with utmost caution. Although linear models exist for essentially all the subsystems of the reflex arc, they cannot be "wired" together to produce a more complete and general model. In biological systems, the whole is considerably more than the sum of its parts and we cannot yet identify, let alone understand or even describe, the many complex and subtle differences that exist.

#### ACKNOWLEDGMENT

This work was supported in part by the National Science Foundation Grant ENG - 7603754 and by NIMHDS grant NS - 00196.

REFERENCES

1. Trukoczy, A., Baldi, T., and Malestic, M., "A Dynamic Model of the Ankle Joint under Functional Electrical Stimulation in Free Movement and Isometric Conditions", J. Biomechanics, Vol. 9, pp. 509-519, 1976.
2. - Functional Neuromuscular Stimulation (report of a workshop), Sitting and Standing Position at Low Frequencies", Human Factors, Vol. 4, pp. 227-253, 1962.
3. Coermann, R. R., "The Mechanical Impedance of the Human Body in
4. Goldman, D. E., and von Gierke, H. E., "The Effects of Shock and Vibration on Man", Report No: 60-3, Naval Medical Research Institute, Bethesda, 1960.
5. Garg, D. P., and Ross, M. A., "Vertical Mode Human Body Vibration Transmissibility", IEEE Transactions Systems, Man & Cybernetics, Vol. SMC-6, pp. 102-112, 1976.
6. Smith, J. B., and Suggs, C. W., "Dynamic Properties of the Human Head", Journal of Sound and Vibration, Vol. 48, pp. 35-43, 1976.
7. Crowninshield, R., Pope, M. H., Johnson, R., and Miller, R., "The Impedance of the Human Knee", J. Biomechanics, Vol. 9, pp. 529-535, 1976.
8. Reynolds, D. D., and Soedel, W., "Dynamic Response of the Hand-Arm System to Sinusoidal Input", in The Vibration Syndrome, W. Taylor (Editor), pp. 149-168, Academic Press, New York, 1974.
9. Suggs, C. W., "Modelling of the Dynamic Characteristic of the Hand-Arm System", in The Vibration Syndrome, W. Taylor (Editor), pp. 169-186, Academic Press, New York, 1974.
10. Allum, J. H. I., and Young, I. R., "The Relaxed Oscillation Technique for the Determination of the Moment of Inertia of Limb Segments", J. Biomechanics, Vol. 9, pp. 21-25, 1976.
11. Duggan, T. C., and McLellan, D. L., "Measurement of Muscle Tone: A Method Suitable for Clinical Use", Electroencephalography and Clinical Neurophysiology, Vol. 35, pp. 654-658, 1973.
12. Wilke, D. R., "The Relation Between Force and Velocity in Human Muscle", J. Physiology, Vol. 110, pp. 289-290, 1950.
13. Agarwal, G. C., Berman, B. M., and Stark, L., "Studies in Postural Control Systems. Part I: Torque Disturbance Input", IEEE Transactions Systems Science and Cybernetics, Vol. SMC-6, pp. 116-121, 1970.
14. Wieneke, G. H., and Denier van der Gon, J. J., "Variations in the Output Impedance of the Human Motor System", Cybernetik, Vol. 9, pp. 159-178, 1974.
15. Joyce, G. C., Back, P. M. H., and Ross, H. F., "The Forces Generated at the Human Elbow Joint in Response to Imposed Sinusoidal Movements of the forearm", J. Physiology, Vol. 240, pp. 351-374, 1974.
16. Agarwal, G. C., and Gottlieb, G. L., "Oscillation of the Human Ankle Joint in Response to Applied Sinusoidal Torque on the Foot", J. Physiology, Vol. 268, pp. 151-176, 1977.
17. Manard, A., and Stein, R. S., "Determinants of the Frequency Response of Isometric Soleus Muscle in the Cat Using Random Nerve Stimulation", J. Physiology, Vol. 229, pp. 275-296, 1973.
18. Reva, P., and Stein, R. S., "Frequency Response of Human Soleus Muscle", J. Neurophysiology, Vol. 39, pp. 786-793, 1976.
19. Poppele, R. E., and Beeman, R. J., "Quantitative Description of Linear Behavior of Mammalian Muscle Spindles", J. Neurophysiology, Vol. 33, pp. 59-72, 1970.
20. Bassan, Z., and Hook, J. C., "Analysis of the Response Properties of De-efferented Mammalian Spindle Receptors Based on Frequency Response", J. Neurophysiology, Vol. 38, pp. 663-672, 1975.
21. Poppele, R. E., and Terzuolo, C., "Thyrotropic Reflex: Its Input-Output Relation", Science, Vol. 159, 743-745, 1968.
22. McRuer, D. T., Magdaleno, R. E., and Moore, G. P., "A Neuron-mechanical Actuation System Model", IFAC Symposium on Technical and Biological Problems in Cybernetics, Yerevan, USSR, 1969.
23. Gordon, A. M., Burley, A. F., and Julian, F. J., "The Variation in Isometric Tension with Sarcomere Length in Vertebrate Muscle Fibers", J. Physiology, Vol. 184, pp. 170-192, 1966.
24. Bendat, J. S., and Piersol, A. G., Random Data: Analysis and Measurement Procedures, Wiley, New York, 1971.
25. Hopkins, M. T., "Identification of the Human Able Control System", Ph.D. Thesis, University of Illinois at Urbana, 1969.

26. Joyce, G. C., and Rack, P. M. H., "Isotonic Lengthening and Shortening Movements of Cat Soleus Muscle", *J. Physiology*, Vol. 204, pp. 475-491, 1969.
27. Stark, L., *Neurological Control Systems: Studies in Bioengineering*, Plenum Press, New York, 1968.
28. Ishida, A., and Umetani, Y., "A Model of the Stretch Reflex Arc for the Upper Arm with Respect to Tremor", in *1973 Biomechanics Symposium*, edited by Y. C. Fung and J. A. Brighton, pp. 51-52, ASME, New York, 1973.
29. Gottlieb, G. L. and Agarwal, G. C., "Two Methods of Measuring the Dynamic Behavior of the Stretch Reflex in Man", Proc. San Diego Biomedical Symposium, Feb. 2-4, 1977.
30. Coggshall, J. D. and Bekey, G. C., "EMG - Force Dynamics in Human Skeletal Muscles", *Medical & Biological Engineering*, Vol. 8, pp. 265-270, 1970.
31. Crochetiere, W. J., Vodovnik, L., and Reswick, J. B., "Electrical Stimulation of Skeletal Muscle - A Study of Muscle as an Actuator", *Medical & Biological Engineering*, Vol. 5, pp. 111-125, 1967.
32. Gottlieb, G. L., and Agarwal, G. C., "Dynamic Relationship Between Isometric Muscle Tension and the Electromyogram in Man", *J. Applied Physiology*, Vol. 30, pp. 345-351, 1971.

TABLE I

SUBJECT	BIAS (Kg.m.)	J (N.m.sec <sup>2</sup> /rad)	B			C (rad/sec)	$\omega_n$ (rad/sec)
			K	R	θ		
GCA	0.0	0.0164	0.362	22.1	0.301	36.7	
	0.1	0.0152	0.433	26.3	0.343	41.6	
	0.2	0.0155	0.461	26.8	0.357	41.6	
	0.4	0.0164	0.388	32.6	0.265	44.6	
	0.6	0.0158	0.447	36.2	0.296	47.8	
	0.8	0.0156	0.509	39.1	0.326	50.1	
	1.0	0.0147	0.561	45.0	0.345	55.3	
	1.2	0.0146	0.588	52.6	0.336	60.0	
GLG	0.0	0.0191	0.234	14.8	0.220	27.8	
	0.25	0.0172	0.364	25.3	0.274	38.6	
	0.5	0.0174	0.384	37.7	0.237	46.5	
	0.75	0.0182	0.401	43.8	0.225	49.1	
	1.0	0.0179	0.631	56.2	0.315	56.0	
BMP	0.0	0.0178	0.333	14.9	0.323	29.0	
	0.25	0.0146	0.574	24.1	0.483	40.7	
	0.5	0.0174	0.488	34.6	0.315	44.6	
	0.75	0.0190	0.470	44.6	0.255	48.5	
	1.0	0.0218	0.539	54.9	0.246	50.2	
	1.25	0.0210	0.609	62.5	0.266	54.5	
Foot Plate	-	0.0098	0.158	1.27	0.712	11.4	
	-	0.0096	0.131	1.14	0.627	10.9	

Mechanical Parameters of the Ankle Joint at different levels of voluntary contraction of the leg muscles acting about the ankle against a constant bias torque.

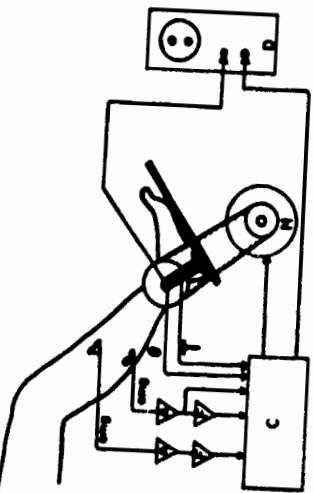


Figure 1  
A schematic of the apparatus used for the measurement of the ankle joint compliance. The components are: D.C. torque motor (M) driven by a Bulova power amplifier. Electromyograms are measured using disc electrodes placed over the bellies of the soleus and anterior tibial muscles. EMG amplifier (A) are differential amplifiers (bandwidth 60-600 Hz), filters (F) are third order averaging (10 msec averaging time), display oscilloscope (D) and digital computer (C).

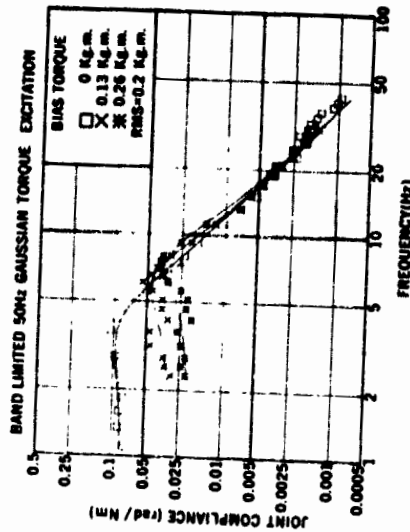


Figure 3  
Effective compliance of the ankle joint measured in rad/N.m. as a function of the drive frequency at three bias torque levels. The solid lines are for a best-fit, second order model.

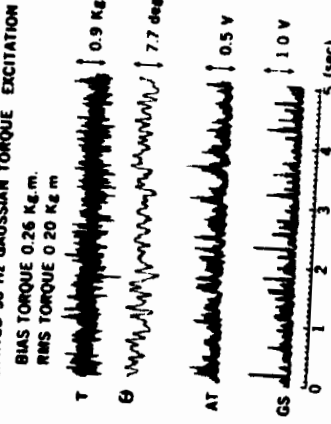


Figure 2  
Response of the ankle joint and muscles in response to a band-limited 50 Hz Gaussian torque input. The four traces are the motor torque ( $\tau$ ), foot angle ( $\theta$ ), anterior tibial muscle EMG (AT) and soleus muscle EMG (GS). The EMG scales are in volts after amplification, rectification and filtering of the surface EMG.

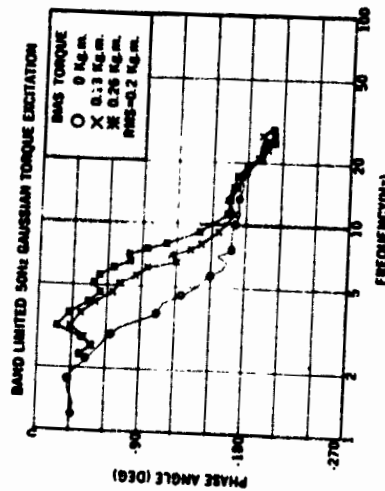


Figure 4  
The phase relationship corresponding to the compliance data in Figure 3.

ORIGINAL PAGE IS  
OF POOR QUALITY

470

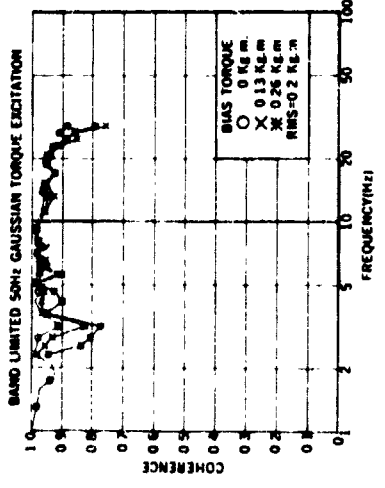


Figure 5  
The coherence functions for the experiment in Figure 3. For the relaxed limb, the coherence was close to unity down to 1 Hz. With nonzero bias torque, the coherence values fell sharply below 2 Hz. Between 2 and 25 Hz, the coherence values are close to one indicating that the system appears fairly linear and noise free.

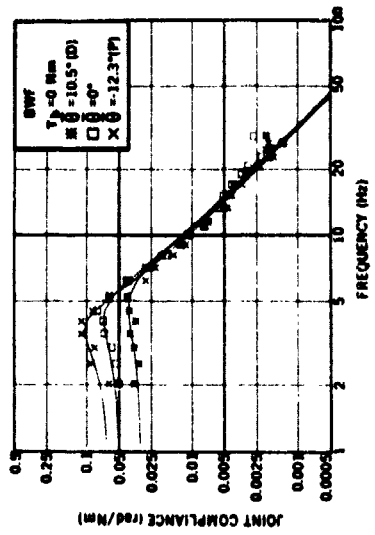


Figure 5  
The coherence functions for the experiment in Figure 3. For the relaxed limb, the coherence was close to unity down to 1 Hz. With nonzero bias torque, the coherence values fell sharply below 2 Hz. Between 2 and 25 Hz, the coherence values are close to one indicating that the system appears fairly linear and noise free.

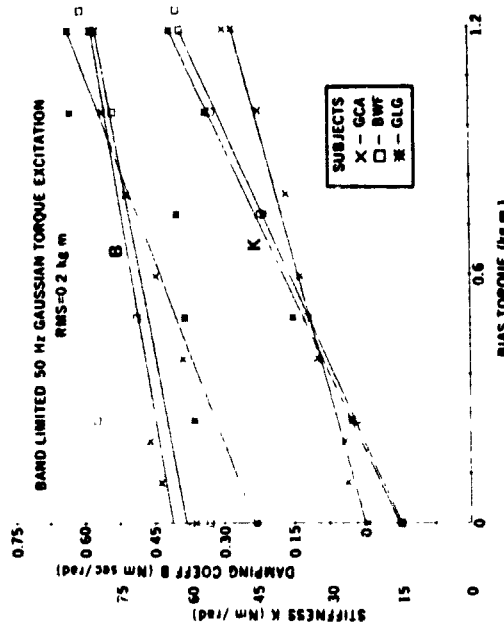


Figure 6  
The joint viscous coefficient ( $B$ ) in N.m.sec/rad and the stiffness ( $K$ ) in N.m/sec/rad as a function of the bias torque (average muscle activation) in N.m. with first order regression lines. The equations of these lines and the correlation coefficients are given in the text.

Figure 7  
Effective compliance of the ankle joint measured in rad/N as a function of the drive frequency with zero bias torque and three values of mean joint angle ( $P$  = Dorsal,  $T_0$  = Plantar). The solid lines are for a best-fit, second order model.

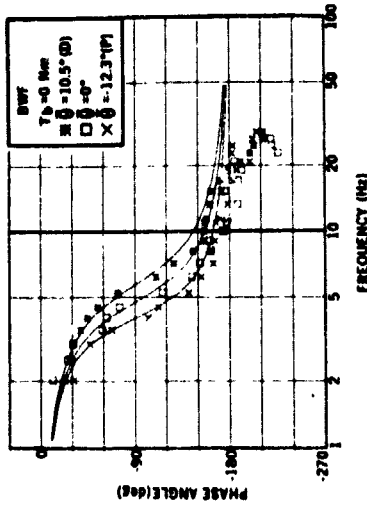
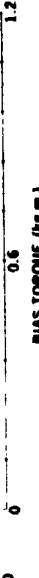


Figure 8  
The phase relationship corresponding to the compliance data in Figure 7. The change in the phase angle near 18 Hz indicates a higher order system dynamics.



ORIGINAL PAGE IS  
OF POOR QUALITY

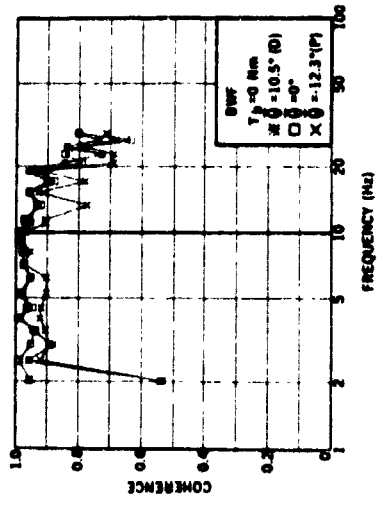


Figure 9  
The coherence functions for the experiment in Figure 7.

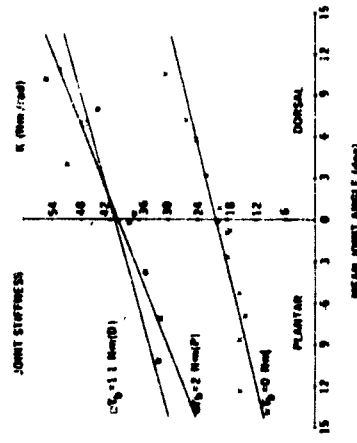


Figure 10  
The joint stiffness in Nm/rad as a function of the mean joint angle with three different bias torques. The equations of the first order regression lines and the correlation coefficients are given in the text.